Fabrication of Halloysite@polypyrrole Composite Particles and Polypyrrole Nanotubes on Halloysite Templates

Yushan Liu, Haiming Nan, Qiang Cai, Hengde Li

Key Laboratory for Advanced Materials of Ministry of Education and Department of Materials Science and Engineering, Tsinghua University, Beijing 100084, People's Republic of China

Received 18 March 2010; accepted 1 August 2010
DOI 10.1002/app.34125
Published online 7 February 2012 in Wiley Online Library (wileyonlinelibrary.com).

ABSTRACT: Halloysites (HNTs) core-polypyrrole(PPy) shell composite particles were fabricated by *in situ* oxidative polymerization of the pyrrole monomer absorbed HNTs nanotubes, obtained by the dispersion of HNTs in acid aqueous solution of pyrrole with ultrasonic irradiation and magnetic stirring, by using ammonium persulfate as oxidant. Further more, the PPy nanotubes were obtained after the removal of HNTs template by hydrochloric acid/hydrofluoric acid mixture. Both the nanocomposite particles and the PPy nanotubes were characterized by FTIR, X-ray diffraction, thermogravimetric analysis, scanning electron microscopy (SEM), and transmission electron microscopy (TEM). The SEM and the TEM images showed that the PPy is covered over the HNT surface forming the HNT@PPy hybrids, and all of the nanotubes have a uniformly inner diameter of 40 nm. The outer diameter and the tubular thickness were determined by the weight ratio of (HNTs template)/(pyrrole monomer). When the amount of pyrrole added is <0.75 mL, no tubular PPy formed any more. The electrical conductivities of the HNT@PPy composite particles and the PPy nanotubes/particles were also investigated. © 2012 Wiley Periodicals, Inc. J Appl Polym Sci 125: E638–E643, 2012

Key words: halloysite; polypyrrole; nanocomposites; core-shell; tubular polypyrrole

INTRODUCTION

The fabrication of intrinsic conducting polymers with various dimensions of nanostructure materials has attracted much attention, because they have the advantages of low-dimensional organic conductors with high surface area and might be used as polymeric conducting molecular wires,[1] light-emitting devices,[2] and chemical and molecular sensors.[3,4] One of these conductive polymers, polypyrrole (PPy), has been received a lot of interest for its high conductivity, good environmental stability, and hitherto a large variety of applications because of the merits of the convenience of the preparation method and cheapness of the monomer recently.[5,6] PPy has been widely studied for biomedical applications, such as biosensors, drug delivering vehicles, and nerve tissue engineering scaffolds.[7] The PPy with different nanostructures is of great significance in the research of this conducting polymer because of their special properties and promising applications in nanodevices.[8] Tubular PPy can be synthesized via self-assembly of monomer and soft templates and hard templates.[9] Some molecules are used as the soft templates in the self-assembly system, such as cetyltrimethylammonium bromide (CTAB)[10] and polymers[11]. In the hard template approach, the target material is precipitated or polymerized on the surface of the template to form core-shell structure.[12,13] Hollow nanocapsules or nanotubes can be obtained[12] after the removal of the hard template. The greatest advantage of the "hard" template approaches is that the inner diameters of the nanotubes could be controlled by the sizes of the hard templates used.

Halloysite (HNT) is one of the naturally occurring clays with tubular shape and can be mined from natural deposits in countries such as China, America, Brazil, and France. Its formula is $Al_2Si_2O_5(OH)_4{\cdot}2H_2O$. It is defined as a two-layered aluminosilicate, chemically similar to kaolin, which has a predominantly hollow tubular structure in the submicrometer range.[14,15] As for most natural clays, the size of HNT particles vary from hundred nanometers to several micrometers in length and have an inner diameter of 10–150 nm depending on the different deposits. A large amount of active agents can be entrapped into the inner lumen of the HNT nanotubes, for example: drugs,[16] nicotinamide adenine dinucleotide,[17] marine biocides,[18] followed by their retention and release. Recently, HNT was also used as adsorbents,[19,20] nanocomposites,[21–25] biomimetic nanoreactors,[26] and nanotemplates or nanoscale reaction vessels instead of carbon nanotubes or boron nitride nanotubes.[27,28]

Correspondence to: Q. Cai (caiqiang@mail.tsinghua.edu.cn).
Contract grant sponsor: China Postdoctoral Science Foundation; contract grant number: 20090450347.

In this article, we report the fabrication of PPy nanotubes with HNT nanotubes as hard template. The HNTs could be etched by HF/HCl solution, because of the outmost surface with the properties of SiO_2 and properties of the inner cylinder core with Al_2O_3.[29] So, the PPy nanotubes were obtained after removal of the template when the HNTs@PPy was fabricated via *in situ* oxidative polymerization. The effect of the different amounts of pyrrole monomer to the formation of the PPy nanotubes was also discussed. No tubular PPy could be obtained any more when the amount of pyrrole added is <0.75 mL.

EXPERIMENTAL

Raw materials

HNT clay was obtained from Hebei Province, China.

Pyrrole (analytical grade reagent, Xi'an Reagent Co., Xi'an, China) was freshly distilled under pressure before use.

Concentrated hydrochloric acid (HCl), hydrofluoric acid (HF), and ammonium persulfate (APS) were analytical grade reagents received from Tianjin Chemical Co. (Tianjin, China) and used without further purification as received.

Deionized water was used throughout.

Preparation of the core-shell structure halloysite@polypyrrole composite particles

HNT was pretreated by the followed procedure: 250-g raw HNT clay and 500-mL water were mixed and milled with SF400 type wit sand-grinding dispersing machine at 4000 rpm for 2 h. The HNT nanotubes suspension was centrifugated (3000 rpm for 3 min) to throw away the deposit. The HNT was dried in vacuum oven for further experiments[20] and then treated in flask as following:

HCl (6 mL) was added into 450-mL distilled water; 3.0-g HNT was dispersed into the mixture in ultrasonic bath for 30 min, and a stable suspension was obtained. Then certain amounts of pyrrole (1.5, 1.0, 0.75, or 0.5 mL) were added into the suspension. The mixture was stirred under magnetic stirring for one night, and the suspension was used for further experiments directly. Then 100 mL of the acidic aqueous solution of APS [containing according amounts of APS (6.80 g, 4.54 g, 3.4 g, 2.27 g, and concentrated HCl 1.00 mL) was added dropwise into the mixtures within 30 min with magnetic stirring in an ice–water bath (Table I). The mixture was stirred for 12 h with magnetic stirring. After the polymerization, the mixtures were centrifugated, and the black powders were obtained. The products were washed by water for several times until neutral and dried under vacuum at 40°C overnight.

TABLE I
Preparation Conditions for the HNTs@PPy Nanocomposites

Samples	HNTs (g)	Pyrrole (mL)	APS (g)
HNTs@PPy sample-1	3	1.5	6.80
HNTs@PPy sample-2	3	1.0	4.54
HNTs@PPy sample-3	3	0.75	3.4
HNTs@PPy sample-4	3	0.5	2.27

Preparation of the tubular polypyrrole nanotubes

The HNTs@PPy composite particles obtained (1.0 g) were dispersed in 100-mL water containing concentrated HCl 10 mL and concentrated HF 10 mL with ultrasonic irradiation for 30 min and then immerged overnight. The PPy nanotubes produced were washed with water for several times until neutral and dried under vacuum at 40°C overnight.

Characterization and analysis

The chemical structure of HNTs, HNTs@PPy composites, and the PPy nanotubes were conducted by recording infrared spectra using Bruker IFS 66 v/s infrared spectrometer in the range of 400–4000 cm^{-1} with the resolution of 4 cm^{-1}. The KBr pellet technique was adopted to prepare the sample for recording the IR spectra.

The X-ray diffraction (XRD) patterns were recorded in the range of $2\theta = 3.0°$ to 80° by step scanning with a Rigaku D/max-IIIA diffractometer (Japan). Nickel-filter Cu Ka radiation ($l = 0.15418$ nm) was used with a generator voltage of 40 kV and a current of 30 mA. Each sample was scanned from (2θ) with a scanning speed of 1°/min.

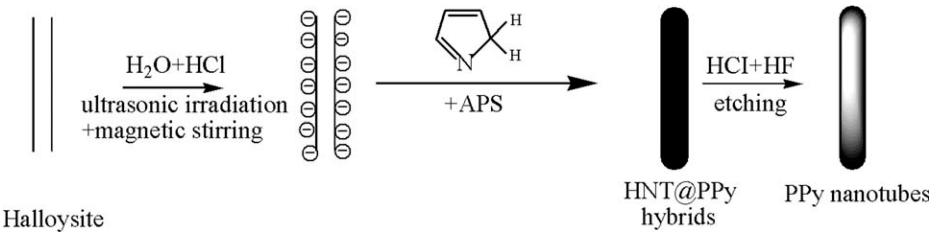

Scheme 1 The formation mechanism of the core-shell HNTs@PPy hybrids and PPy nanotubes/particles.

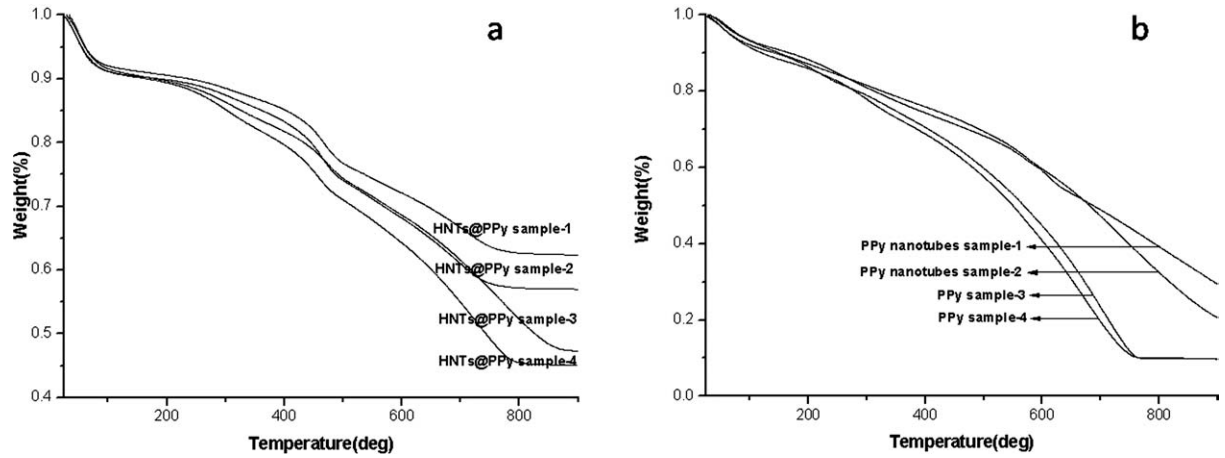

Figure 1 TGA curves of the (a) HNTs@PPy composite particles and (b) the PPy nanotubes.

The surface morphologies of particles were observed using field-emission scanning microscope (SEM.Jeol JSM-6301F).

The transmission electron microscopy (TEM) observation was performed on a JEOL JEM-2010F electron microscope (Japan) operating at 200 kV. The powders were dispersed in water in an ultrasonic bath for 5 min and then deposited on a copper grid covered with a perforated carbon film.

The thermogravimetric analysis (TGA) was conducted on a TA Instrument TGA-2050 with the temperature range from room temperature to 900°C under N_2.

The electrical conductivities of the HNTs@PPy composite particles and PPy nanotubes prepared with different HCl concentrations were measured using SDY-4 Four-Point Probe Meter at ambient temperature employing the method on a pressed pellet according to the formula[29]:

$$\sigma = 1/\rho = V/I \times F(D/S) \times F(W/S) \times W \times Fsp,$$

where σ referred to electrical conductivity, V is the voltage, I is the current, D is the diameter of the pellets, W is the thickness of the pellets, S is the average space between the probes, $F(D/S)$ is the amendatory coefficient of the diameter of the pellets, $F(W/S)$ is the amendatory coefficient of the thickness of the pellets, and Fsp is the amendatory coefficient of the space between the probes. The pellets were obtained by subjecting the powder sample to a pressure of 30 MPa. The reproducibility of the result was checked by measuring the resistance three times for each pellet.

RESULTS AND DISCUSSION

In situ oxidative polymerization

In the solution at a low pH, the negative charges are introduced to the host HNTs nanotubes' outmost surface, and the strong electrostatic force works

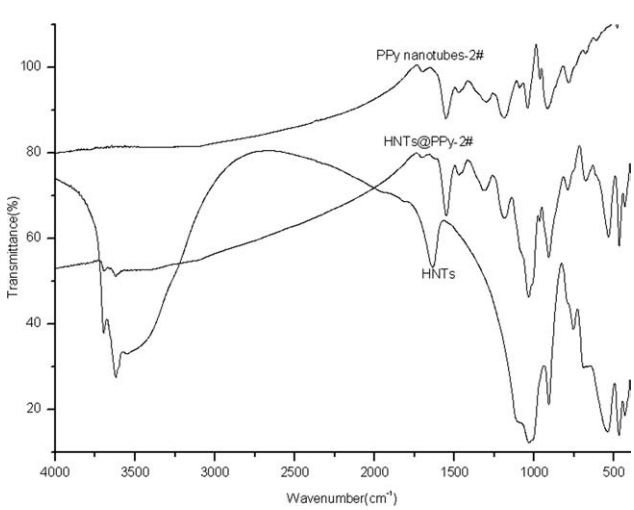

Figure 2 FTIR spectra of the HNTs, HNTs@PPy hybrids, and PPy nanotubes.

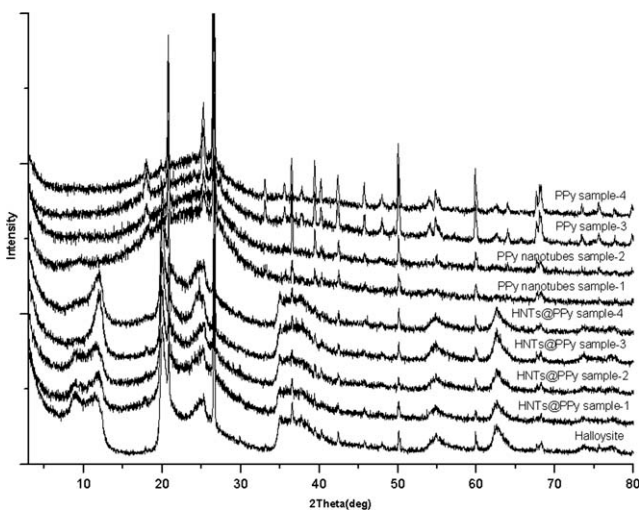

Figure 3 XRD patterns of the HNTs, HNTs@PPy, PPy nanotubes, and PPy.

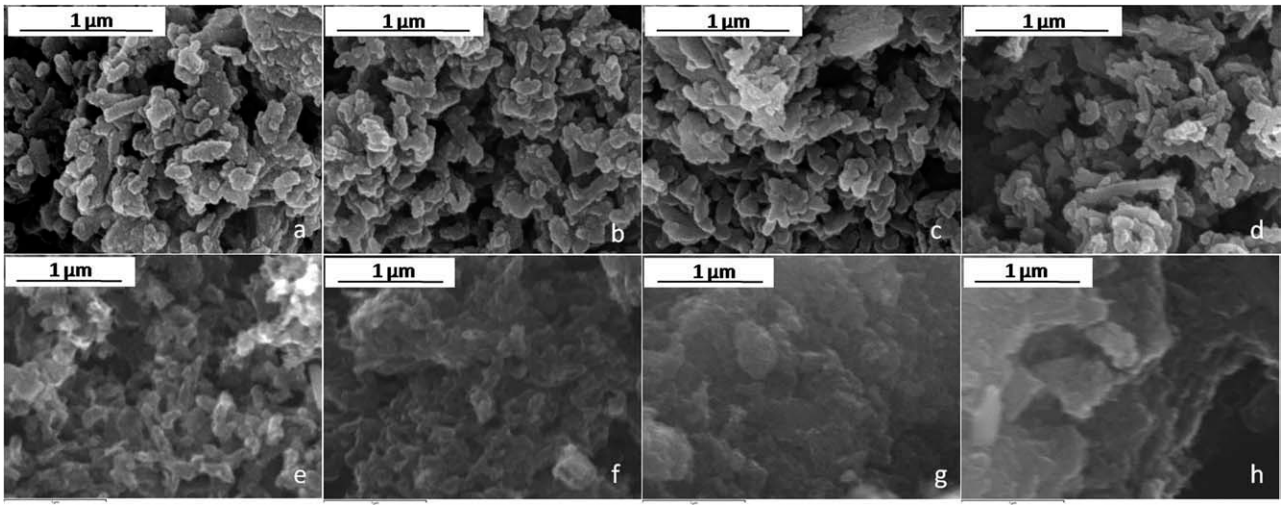

Figure 4 The SEM images of the HNTs@PPy hybrids and the PPy nanotubes. (a) HNTs@PPy sample-1; (b) HNTs@PPy sample-2; (c) HNTs@PPy sample-3; (d) HNTs@PPy sample-4; (e) PPy nanotubes sample-1; (f) PPy nanotubes sample-2; (g) PPy sample-3; and (h) PPy sample-4.

between the negative host and the positive polymer. The PPy can be absorbed to the HNTs nanotubes' surface and encapsulated the tubes to form the core-shell structure hybrids. After etching by HF/HCl solution, the HNTs templates were removed, and the tubular PPy was obtained. The mechanisms could be shown schematically as Scheme 1.

It could be concluded that almost all the pyrrole monomers were oxidative polymerized into the PPy layers from the TGA curves of the HNTs@PPy composite particles prepared with different amounts of pyrrole monomer [Fig. 1(a)]. The first stage close to 130°C was mainly due to the removal of the HCl doped and moisture. The PPy of the HNTs@PPy hybrids started to decompose at about 250°C,[30] which is not very different from normal PPy nanotubes shown in Figure 1(b). The different amount of residue [Fig. 1(a)] was caused by the different ratios of pyrrole monomer to HNTs. There also have some amounts of residue, shown in Figure 1(b), that might be caused by the residues of the HNTs.

Spectroscopic analyses

The FTIR spectra of the raw HNT, HNTs@PPy hybrids, and the PPy nanotubes were shown in Figure 2. The main characteristic peaks of the HNTs@PPy hybrids are assigned as follows: the bands at 1554 and 1474 cm^{-1} are attributed to typical pyrrole rings vibration; the bands at 1307, 1193,

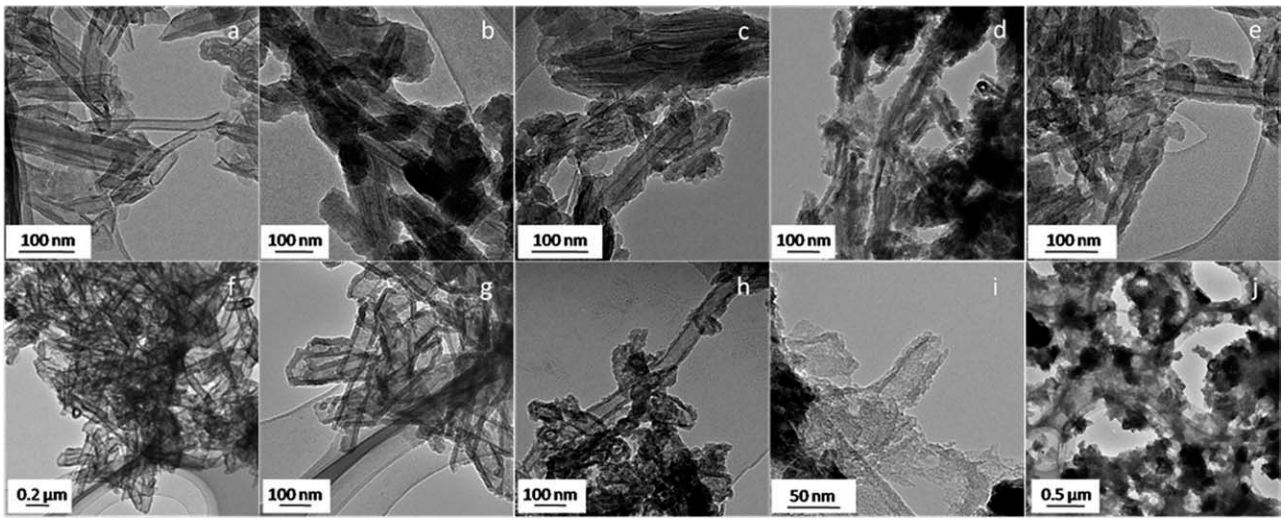

Figure 5 The TEM image of halloysite nanotubes, HNTs@PPy hybrids, and PPy nanotubes. (a) Halloysite nanotubes; (b) HNTs@PPy sample-1; (c) HNTs@PPy sample-2; (d) HNTs@PPy sample-3; (e) HNTs@PPy sample-4; (f) PPy nanotubes sample-1;(g, enlarged) PPy nanotubes sample-1; (h) PPy nanotubes sample-2; (i) PPy sample-3; and (j) PPy sample-4.

TABLE II
Descriptions of the PPy Nanotubes and PPy

Samples	Morphology	Inner diameter (nm)	Thickness of PPy layer (nm)
PPy nanotubes sample-1	Tubular	About 40 nm	About 10 nm
PPy nanotubes sample-2	Tubular	About 40 nm	About 8 nm
PPy sample-3	Tubular and particles	About 40 nm	About 5 nm
PPy sample-4	Particles	Without inner diameter	Without thickness

and 1036 cm^{-1} are attributed to =C—H in-plane vibration, and the bands at 791 and 910 cm^{-1} are attributed to =C—H out-of-plane vibration.[31] In the spectrum of PPy nanotubes, the bands at 3710, 3650, 1640, 1040, 910, 750, 550, and 460 cm^{-1} disappeared. It showed that the HNTs templates were etched after the treatment with the HF/HCl mixture.[31]

Figure 3 shows the XRD patterns of HNT nanotubes, HNTs@PPy composites, and PPy nanotubes. The peak at about $2\theta = 25^\circ$ is a characteristic peak of PPy.[32] It indicated that the PPy encapsulate the HNTs. After the etching of HNTs by HCl/HF mixture, the XRD peak at about 13° disappeared; it indicated that the crystal structures of the HNTs were destroyed.[25] It also indicated that the HNTs templates were removed, and only tubular PPy obtained.

Morphological analysis

The morphologies of the HNTs@PPy hybrids with core-shell structure were shown in the SEM [Fig. 4(a–d)]. The morphologies of the particles prepared with different amounts of pyrrole monomer were similar. The HNTs were encapsulated very well by PPy layer. The PPy nanotubes obtained after the removal of HNTs were shown in Figure 4(e,f). We found that there are no PPy nanotubes in Figure 4(g,h) because of the less amounts of pyrrole monomers.

Compared with that of the raw HNT nanotubes in Figure 5(a), direct evidence for the formation of the PPy layers on the surfaces of the HNTs is provided in the TEM images [Fig. 5(b–e)]. It was observed that the morphologies of the HNTs@PPy particles prepared with different amounts of PPy monomer were similar but with a little difference in the thickness of the PPy layers. The adsorption amount of the PPy molecules onto the surfaces of the HNT nanotubes might affect the thickness of the layer. The more monomers added the more PPy molecules adsorbed onto the surfaces of the HNTs. It is clear from the images that the HNTs@PPy particles [Fig. 5(b–e)], the inner hollow cavity of the HNTs@PPy hybrids, remained at about 10 nm as the raw HNTs, but the outer diameters of the HNTs@PPy hybrids decreased from about 60 nm [Fig. 5(b)] to about 50 nm [Fig. 5(e)]. It indicated that the PPy layer coated only onto the outer surfaces of the HNTs, and the thickness of the layers decreased by the decrease amounts of the pyrrole monomers added.

The TEM images of PPy were shown in Figure 5(f–j) after etching the HNTs by the HF/HCl solution. The images of PPy nanotube 1.5 mL are shown in Figure 5(f,g). It is clear that the nanotubes were uniform with inner diameter of 40 nm. The thickness of the PPy shell layer in the PPy nanotubes is about 10–15 nm. The image of tubular PPy with 1-mL pyrrole monomer was shown in Figure 5(g), and the tubular PPy with thinner shell and inner diameter of 40 nm was obtained after removal of the HNTs. Very few tubular PPy can be found when 0.75-mL pyrrole monomer added. The nanotube in Figure 5(h) seems very weak and easy to be destroyed. No tubular PPy was found in Figure 5(i) because of the little amounts of pyrrole monomer added. When too little monomer added, the PPy shell is too weak to maintain the tubular shape after the etching of HNTs by HCl/HF mixtures, and no tubular PPy obtained any more (Table II). The thick PPy layer is favorable to form the tubular PPy.

Electrical conductivity

The electrical conductivities of the HNTs@PPy composite particles prepared with different amounts of

TABLE III
The Effect of the Pyrrole Monomer Added in the Dispersion on the Electrical Conductivity of the HNTs@PPy Composites

Samples	Pyrrole added (mL)	σ (S cm^{-1})
HNTs@PPy 1#	1.5	0.112
HNTs@PPy 2#	1.0	8.75×10^{-2}
HNTs@PPy 3#	0.75	2.809×10^{-2}
HNTs@PPy 4#	0.5	5.91×10^{-3}

TABLE IV
The Effect of the Pyrrole Monomer Added on the Electrical Conductivity of the PPy Nanotubes

Samples	Pyrrole added (mL)	σ (S cm^{-1})
PPy nanotubes 1#	1.5	0.113
PPy nanotubes 2#	1.0	0.101
PPy nanotubes/particles 3#	0.75	0.069
PPy particles 4#	0.5	0.061

pyrrole monomer added in the mixture were given in Table III. It could be found that the HNTs@PPy composites exhibited good electrical conductivities. Different from the other PPy/silicate clays intercalative composites, here the PPy molecules were adsorbed onto the surfaces of the HNTs nanotubes to form the core-shell structure particles with conductive PPy shells. So, the better electrical conductivities were achieved. The HNTs@PPy composite particles prepared with more pyrrole monomer showed the better electrical conductivities for the thicker PPy layer than the particles prepared with less pyrrole monomer. The electrical conductivities of PPy obtained by etching the template were also shown in Table IV. The electrical conductivities of the PPy nanotubes/particles obtained after the removal of HNTs template by HCl/HF mixture were better than the HNTs@PPy composite particles, because of the poor electrical conductivity of HNTs. There also have some differences between the electrical conductivities of the PPy nanotubes/particles and that may be caused by the residues of the HNTs.

CONCLUSIONS

The preparation of the HNTs@PPy composite particles were conducted via *in situ* oxidative polymerization. The fabrication of the PPy nanotubes was achieved via the removal of the HNT templates by HF/HCl. It was found that the amounts of pyrrole monomer had no effect on the morphologies of the HNTs@PPy but the thickness of the PPy layers. The thickness of the layers was determined by the amounts of the pyrrole monomer added. When the more monomers added, the thicker layer is obtained. The proper amount of the monomer is favorable to form the uniform nanotubes with inner diameter of 40 nm. When the pyrrole monomer added is <0.75 mL, the PPy layer is not thick enough, and the PPy nanotubes cannot be obtained any more.

References

1. Wu, C. G.; Bein, T. Science 1994, 264, 1757.
2. Liang, L.; Liu, J.; Windisch, C. F.; Exarhos, G. J.; Lin, Y. Angew Chem Int Ed 2004, 41, 3665.
3. Liu, H.; Kameoka, J.; Czaplewski, D. A.; Craighead, H. G. Nano Lett 2004, 4, 671.
4. Virji, S.; Huang, J.; Kaner R. B.; Weiller, B. H. Nano Lett 2004, 4, 491.
5. Yan, F.; Xue, G.; Wan, G. F. J Mater Chem 2002, 12, 2606.
6. Li, F. L.; Yan, F.; Xue, G. J Appl Polym Sci 2004, 91, 303.
7. Lee, J. Y.; Lee, J. W.; Christine, E. S. J R Soc Interf 2009, 6, 801.
8. Zhang, Z. M.; Sui, J.; Zhang, L. J.; Wan, M. X.; Wei, Y. Adv Mater 2005, 17, 2854.
9. Liu, P.; Zhang, L. Crit Rev Solid State Mater Sci 2009, 34, 75.
10. Wu, Q. F.; He, K. X.; Mi, H. Y.; Zhang, X. G. Mater Chem Phys 2007, 101, 367.
11. Zhou, F.; Liu, W.; Hao, J.; Xu, T.; Chen, M.; Xue, Q. Adv Funct Mater 2003, 13, 938.
12. Liu, P. In Recent Research Developments in Applied Polymer Science; Pandalai, S. G., Eds.; Research Signpost: India, 2008, 4, 351.
13. Khan, M. A.; Armes, S. P. Adv Mater 2000, 12, 671.
14. Singh, B.; Gilkes, R. Clays Clay Miner 1992, 40, 212.
15. Remskar, M. Adv Mater 2004, 16, 1497.
16. Levis, S. R.; Deasy, P. B. Int J Pharm 2003, 253, 145.
17. Lvov, Y.; Price, R.; Gaber, B.; Ichinose, I. Colloids Surf A 2002, 198, 375.
18. Price, R.; Gaber, B.; Lvov, Y. J Microencapsulation 2001, 18, 713.
19. Zhao, M. F.; Liu, P. Microporous Mesoporous Mater 2008, 112, 419.
20. Ye, Y. P.; Chen, H. B.; Wu, J. S.; Ye, L. Polymer 2007, 48, 6426.
21. Zheng, Y. A.; Wang, A. Q. J Macromol Sci: Pure Appl Chem 2010, 1, 33.
22. Liu, M. X.; Guo, B. C.; Du, M. L.; Cai, X. J.; Jia, D. M. Nanotechnology 2007, 18, 455703.
23. Liu, M. X.; Guo, B. C.; Zou, Q. L.; Du, M. L.; Jia, D. M. Nanotechnology 2008, 19, 205709.
24. Zhang, L.; Wang, T. M.; Liu, P. Appl Surf Sci 2008, 2091, 255.
25. Shchukin, D. G.; Sukhorukov, G. B.; Price, R. R.; Lvov, Y. M. Small 2005, 1, 510.
26. Antill, S. J. Aust J Chem 2003, 56, 723.
27. Wang, A. P.; Kang, F. Y.; Huang, Z. H.; Guo, Z. C.; Chuan, X. Y. Microporous Mesoporous Mater 2008, 108, 318.
28. The Manual of the SX1934 Four-Point Probe Meter; Suzhou Telecom Instrument Factory: Suzhou, China.
29. Chen, W.; Li, X.; Xue, G.; Wang, Z.; Zou, W. Appl Surf Sci 2003, 218, 215.
30. Zhang, L.; Liu, P. Nanoscale Res Lett 2008, 3, 299.
31. Cheah, K.; Forsyth, M.; Truong, V. T. Synth Met 1998, 94, 215.